RSC Advances




ROYAL SOCIETY OF CHEMISTRY

www.rsc.org/advances

Journal Name

ARTICLE

# Single-crystalline rutile $TiO_2$ nano-flower hierarchical structures for the enhanced photocatalytic selective oxidation from amine to imine

Received 00th January 20xx,
Accepted 00th January 20xx

DOI: 10.1039/x0xx00000x

www.rsc.org/

Jing Bu,[a] Jun Fang,*[,b] Wan Ru Leow,[a] Kaihong Zheng,[a] Xiaodong Chen*[, a]

Single-crystalline rutile $TiO_2$ nano-flower hierarchical structures were synthesized *via* a one-pot solvent-thermal method, it is demontrated to be an ordered three dimensional (3D) hierarchical structures with single-crystalline rutile $TiO_2$ nanorods as its buliding blocks. They exhibited enhanced photocatalytic activity for the selective oxidation from benzylamine to N-benzylidenebenzylamine (N-BIBL) with high yield under visible light irradiation. Such remarkable performance could attribute to the rapid photocharges separation and inhibition of charges recombination due to the unique hierarchical structures of this single-crystalline rutile $TiO_2$ nano-flower. The facilely prepared single-crystalline rutile $TiO_2$ nano-flowers are promising materials in the field of photocatalytic fine chemical conversions and other photocatalytic applications.

## Introduction

$TiO_2$ (titaium dioxide), as one of the typical transition metal oxides, has been widely studied during the past decades due to its low cost, nontoxicity, and high chemical stability, and its application has been extended to various fields, such as photovoltaic cells,[1] photocatalysis,[2] Li-ion battery materials,[3] sensors[4] and so on. Generally, the performances of these materials are highly dependent on their crystal phases, particle sizes and the exposed facets.[5-10] Ruitle $TiO_2$, as one of the common phases of titania, was well investigated in its mophology-control growth, one of the representative examples is the rutile $TiO_2$ nanorods[11] used for DSSCs.[12] Although significant achievements have been made in synthesis of this isolated 1D nanostructure in the past decades, the well controlled synthesis of complex nanostrucutures such as ordered 3D hierarchical nanostructure with both appropriate designed building blocks and well-defined overall shape still remains great challenge. Compared to 1D nano-materials, three dimensional (3D) hierarchically structured counterparts could provide larger suface area, extend dispersion of active sites at different length scales and shorten diffusion path, it could also allow mutiple light reflections and scatterings. All of these could contribute to remarkbaly improved performances of these materials. To date, 3D materials with hierarchical architectures have attracted inceasing attention.[13-17] However, reports on the synthesis of single crystalline rutile $TiO_2$ 3D hierarchical architectures are still rare.[18]

Herein, we report a facile method to synthesize nano-flower-like rutile $TiO_2$ hierarchical structures, the building blocks of such nano-flower structures are single-crystalline rutile $TiO_2$ nanorods. To the best of our knowledge, the novel photocatalytic activity toward the selective oxidation from benzylamine to N-BIBL by this rutile $TiO_2$ nano-flower structure has not been reported yet. Such excellent photocatalytic performance and the rapid synthesis strategy for the single-crystalline rutile $TiO_2$ nano-flower structures offer the great potentials in the synthesis of such 3D ordered hierarchical strucutures and their promising applications in photocatalytic fine chemical conversions.

## Results and Discussion

Fig 1A and Fig 2B are the typical SEM images of the rutile $TiO_2$ nano-flower structure. The as-synthesized materials are composed of substantial nano-flower-like assemblies. The ordered hierarchical nano-structure was obtained with high yield and uniformity, the diameter of the nano-flowers is ca. 1.2 μm, and the building blocks are these radially oriented single nanorods. Fig 1C and Fig 1D show TEM images of the rutile $TiO_2$ nano-flower structure under different magnifications, one nano-flower composed of the nanorods bundles could be observed under TEM in Fig 1C. The HRTEM image in Fig 1D focused on one tip of the nano-flower, the lattice fringe of $d$ = 0.32 nm could be measured in Fig 1D, which could be assigned to rutile $TiO_2$ (110) facet. The SAED pattern present in the inset image of Fig 1D demonstrates that the nano-flowers are single-crystalline, in which the incident electron beam was examined along the [110] zone axis. Thus, TEM and SAED results indicates that the growth direction of

[a] School of Materials Science and Engineering, Nanyang Technological University, 50 Nanyang Avenue, Singapore 639798, Singapore
[b] State Key Laboratory of Materials-Oriented Chemical Engineering, College of Chemical Engineering, Nanjing Tech University, No. 5 Xin Mofan Road, Nanjing 210009 (P.R. China)
E-mail: fangjun@njtech.edu.cn (Jun Fang) Tel: +862583172232
chenxd@ntu.edu.sg (Xiaodong Chen) Tel: +6565137350
Electronic Supplementary Information (ESI) available

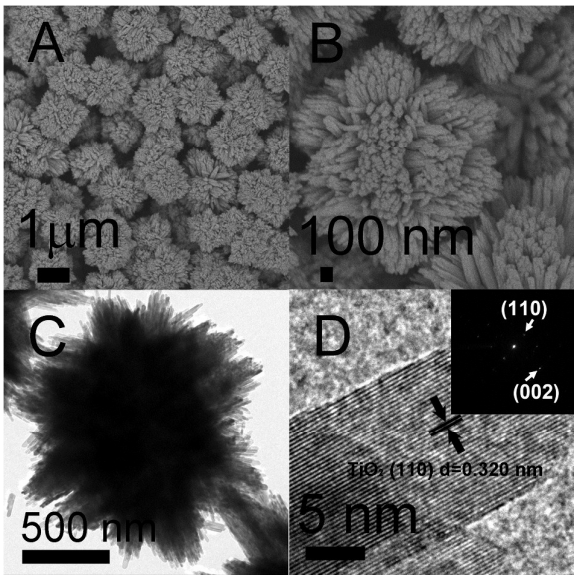


**Fig. 1** (A, B) SEM images of the rutile $TiO_2$ nano-flower structure under different magnification; (C, D) TEM images of the rutile $TiO_2$ nano-flower structure under different magnification; (Inset of D) Selected area electron diffraction (SAED) pattern of rutile $TiO_2$ nano-flower structure.

the nanorod is along [001] axis, so the (110) facet was exposed as the side walls.

Fig 2 shows the typical characterizations of the rutile $TiO_2$ nano-flower structure. The XRD pattern of the rutile $TiO_2$ nano-flower structure is present in Fig 2A. All of the diffraction peaks of the as-synthesized nano-flower structure could be indexed to rutile $TiO_2$ (JCPDS. 21-1276), which indicates that pure rutile $TiO_2$ phase could be synthesized under this solvent-thermal condition. The Raman spectrum of the rutile $TiO_2$ nano-flower structure is shown in Fig 2B. Two characteristic peaks with the Raman shift at 442 $cm^{-1}$ and 606 $cm^{-1}$ could be attributed to the scattering mode of pure rutile $TiO_2$, which are assigned to $E_g$ and $A_{1g}$ mode.[19] No additional Raman bands assigned to other $TiO_2$ phases are observed, which further confirms the single rutile phase feature of the $TiO_2$ samples. Thus the XRD pattern and Raman spectrum of the rutile $TiO_2$ nano-flower structure indicate that the as-synthesized $TiO_2$ nanostructure is composed of pure rutile phase. Fig 2C displays the UV-Vis diffuse reflectance spectrum of rutile $TiO_2$ nano-flower structure, distinct from the typical $TiO_2$ rutile poly-crystalline structure, which presents a mono absorption edge at ca. 400 nm with the band gap ca. 3.0 eV, the spectrum of our rutile $TiO_2$ nano-flower structure exhibits a step in the UV region at ca. 380nm, which implies the unique geometric structure may be present. Furthermore, a plot of the modified Kubelka-Munk function $[F(R_\infty)E]^{1/2}$ *vs* the energy of absorbed light $E$ was used to calculate the values of these two band gaps, and $E_{gap1}$ = 3.0 eV and $E_{gap2}$ = 3.5 eV were obtained. The multiple band gaps presented in the nano-flower structure should be resulted from the quantum confinement of the electrons in these rutile nanorods which are the building blocks for this hierarchical structure. It is reported that for 1D anatase $TiO_2$ nanowires (NWs), when the diameter of the NW

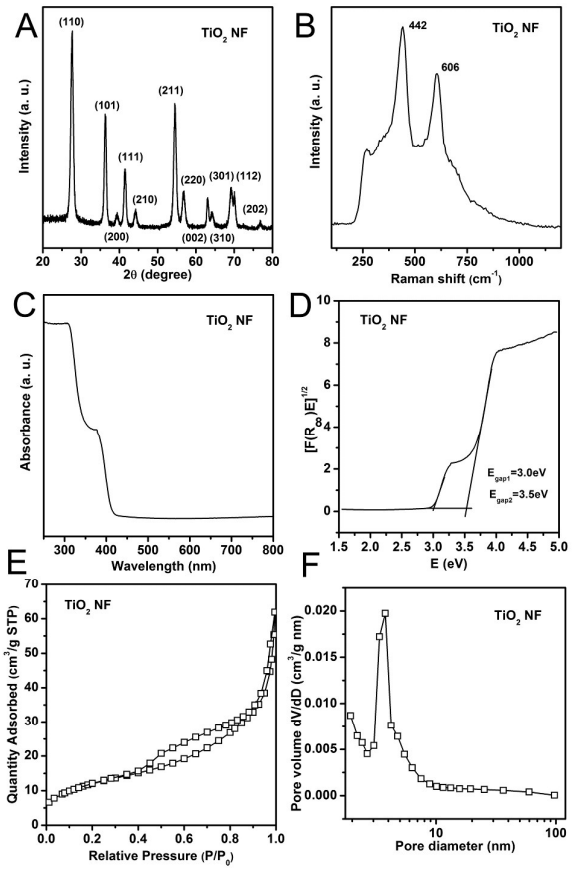


**Fig. 2** (A) XRD pattern of the rutile $TiO_2$ nano-flower structure; (B) Raman spectrum of rutile $TiO_2$ nano-flower structure; (C) UV-Vis diffuse reflectance spectrum of rutile $TiO_2$ nano-flower structure; (D) Transformed UV-Vis diffuse reflectance spectrum of rutile $TiO_2$ nano-flower structure; (E) The $N_2$ adsorption desorption isotherm of rutile $TiO_2$ nano-flower structure; (F) The pore size distributions of rutile $TiO_2$ nano-flower structure.

reduced to 40 nm, the quantum confinement could occur, along with the arising of multiple band-edge absorptions in UV-Vis spectra for such $TiO_2$ NWs.[20] Due to the similar morphology between the 1D $TiO_2$ NWs and the $TiO_2$ nanorods in this case, which are the building blocks for the nano-flower structure, it is reasonable to deduce that such absorption step in the UV-vis reflectance spectra (Fig 2C) could be attributed to the quantum confinement in our rutile $TiO_2$ nano-flowers. The $N_2$ adsorption desorption isotherm of rutile $TiO_2$ nano-flower structure is shown in Fig 2E, the shape of the isotherm indicates that the rutile $TiO_2$ nano-flower shows mesoporous structures, the hysteresis loop in the isotherms is type H2, which could usually be observed in the pores with narrow necks and wider bodies (ink-bottle pores).[21] Pore size distributions were analyzed with the BJH method from the desorption branch of the isotherm (Fig 2F), The nano-flower structure showed a maximum pore diameter at 4.0 nm. The $N_2$ adsorption desorption isotherm and the pore size distributions of P25 was present in Fig S5, which showed distinct features compared with these of rutile $TiO_2$ nano-flowers.P25 possessed a hysteresis loop of type H3, associated with aggregates of platelike particles giving rise to slitlike pores, and

the pore size distribution was much broadened.Table S1 also summarizes the BET surface area, pore volume, and average pore size calculated from the isotherms both for rutile $TiO_2$ nano-flower structure and P25. Rutile $TiO_2$ nano-flower structure showed much smaller pore size than that of P25 and much narrowed pore size distribution, which suggests the integrity of the nano-flower structure rather than the random packed nanoparticles of P25. And this could play important role in charge diffusion in photocatalytic processes.

Based on the synthesized protocol, several parameters were adjusted to examine their influence on the growth of such hierarchical nanostructures. Non-polar solvent toluene was replaced by polar solvent ethanol, as the result, none of an ordered nanostructure was observed (Fig. S1), implying that the interface between polar and non-polar substances are crucial for the vectorial growth of $TiO_2$ nanorods, and their self-assembly procedure. It is the interface between the trace water in HCl and toluene before the $TiO_2$ crystal nucleus, then the interface between hydrophilic $TiO_2$ and toluene induced the growth of $TiO_2$ nanorods.[12] Specifically, the trace water from the HCl solution is immiscible with the nonpolar toluene, initially, water in HCl was uniformly distributed in toluene phase, forming micro-emulsion. Ti precursor could hydrolyze at the water/toluene interfaces and transform into $TiO_2$ nucleus. After the generation of the crystalline nucleus, a new interface between the hydrophilic $TiO_2$ and toluene is formed, with continuous hydrolysis and subsequent growth-crystallization. HCl used was to slow down the hydrolysis rate of Ti precursor by preserving the low pH value of the solution. Such interface in this micro-emulsion system could not be found in water/ethanol mixture solution as they are totally miscible, and therefore, only random packed nanoparticles with non-uniform size distribution was synthesized (Fig. S1).

Besides the solvent, the influence of surfactant in the synthesis of the hierarchical rutile $TiO_2$ was also examined. In this case, three organic ammonium salts, tetraoctylammonium bromide (TOAB), tetradecyltrimethylammonium bromide (TDAB) and cetyltrimethylammonium bromide (CTAB) were selected for the orientation growth of the $TiO_2$ nanostructure. The morphology of the as-prepared $TiO_2$ samples were shown in Fig. S2, respectively, and the inset images are the molecular structures of these surfactants, accordingly. It could be observed that both TDAB and CTAB could induce the formation of the nano-flower structure, whereas using TOAB as the surfactant, only a large domain with the size over 5 μm was obtained, without any ordered hierarchical structure (Fig. S2A). It is known that TDAB and CTAB both show a long mono-chain structure of carbon, with one hydrophilic (amine group) and one hydrophobic (methyl group) double ends. Therefore, the surfactants prefer to be assembled at the interface of water and toluene, forming a micelle. As the proposed growth mechanism of the nano-flower structure aforementioned, surfactants were selectively adsorbed on $TiO_2$ (110) facet preferentially, lowering down the surface energy of $TiO_2$ (110) facet, promoting the anisotropic growth of the $TiO_2$ nano-flower structure. However, for TOAB surfactant, its molecular structure of branch carbon chains with the absence of two different hydrophilic/hydropobic ends, and its stereo configuration restrained its formation of densed micelle and packed closely at the interface of water/toluene. So the nano-flower structure composed of $TiO_2$ nanorods could be obtained using TDAB and CTAB as the surfactant rather than TOAB.

In this paper, CTAB was selected as the solo surfactant applied for the synthesis of all samples. And the amount of CTAB using in the synthesis process was also evaluated. As shown in Fig. S3, only when the molar ratio between CTAB and Ti precursor achieved 1:1, the nano-flower structure with uniform size distribution could be obtained. Otherwise, when the ratio is less than 1:1, the SEM images of the as-synthesized samples are present in Fig. S3 (Fig. S3A to Fig. S3D). It could be observed that without the fully protection of CTAB for the samples during the synthesis process, the uniform nano-flower structure could not be obtained, both larger aggregates with spherical shape and small bundles of nanorods could be formed (Fig. S3). This indicates CTAB showed significant contribution to the morphology control of the samples, both in the constituent nanostructure of each nano-flower and the highly ordered hierarchical structure in overall scale for all the nano-flowers.

For the effective synthesis, temperature is another crucial parameter, and as shown in Fig. S4, only when the reaction temperature retained at 180 $^{o}$C, the uniform nano-flower structure could be fully grown. With the increasing temperature, to minimize system energy, water in this immiscible water/toluene mixture is diffusing away from the high-energy water/toluene interface, with $Ti^{4+}$ precursor hydrolyzed simultaneously. The higher of the temperature, the faster of the diffusing speed of water. Due to the rapid mass transfer at high temperature during the synthesis process, thinner nanorods bundles could be obtained, rather than the thick nanorods with a short longitudinal length synthesized at low temperature (80 $^{o}$C, Fig. S4A). The samples obtained at the temperature between 80 $^{o}$C and 180 $^{o}$C clearly showed the morphology evolution from thick nanorods to uniform nano-flowers (Fig. S4B to Fig. S4D).

Based on all the characterizations aforementioned, a proposed growth mechanism of the rutile $TiO_2$ nano-flower structure is present in Scheme 1. In this micro-emulsion system composed of water/toluene phase, CTAB was used as the surfactant forming micelles at the interfaces of two phases. Firstly, Ti precursor could hydrolyze at the water/toluene interfaces and transform into $TiO_2$ nucleus, where the trace water are from HCl. It is reported that the interface between two immiscible liquids could guide the growth and assembly of nanoparticles, due to nanoparticles were tended to be trapped at the liquids' interface to minimize the Gibbs free energy of the system.[22] A so-called Pickering emulsion was one of these typical examples which consists of oil, water and nanoparticles at their interface. And in this case, we have demonstrated that the interface between toluene and water played a key role for the formation of $TiO_2$ nano-flower hierarchical structures, especially at the initial stage.

After the generation of the crystalline nucleus, a new interface between the hydrophilic

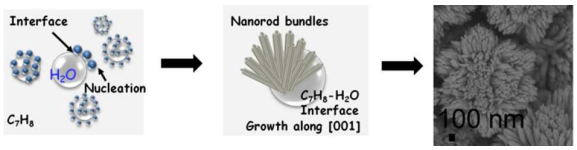


**Scheme 1.** Proposed mechanism of the self-assembly to produce the rutile $TiO_2$ nano-flower hierarchical structures.

$TiO_2$ and toluene is formed, with continuous hydrolysis and subsequent growth-crystallization. The adding of concentrated HCl provided an acidity environment for the synthesis of $TiO_2$ samples, and $TiCl_4$ in the precursor and HCl itself provided plenty of $Cl^-$ ions to the system, the presence of $Cl^-$ ions and low pH value both are demonstrated to favor the growth of the rutile phase rather than anatase phase.[22] Besides, some calculation results have revealed that rutile $TiO_2$ {110} showed the lowest surface energy of 1.78 $J \cdot m^{-2}$ among all the rutile facets.[23] Moreover, in this case, the selective adsorption of $Cl^-$ ions on (110) crystal faces favored the growth of rutile nanorods along the [001] direction. The surfactant CTAB would preferentially enhanced the oriented growth process, with the stabilization of CTAB, $TiO_2$ nanorods showed vectorial growth along [001] direction, mainly exposed (110) facet as the side walls of the nanorods. In this acidic solution, all the nanorods are protonated, after the formation of single thin rutile nanorod, the agglomeration of these nanorods were promoted, which attributed to the hydrogen bonding between neighboured protonated nanorods. So in this case, the rutile nanorods could attach to each other in an oriented fashion to further reduce the surface energy of the system and finally, these nanorods self-assembled into nano-bundles. As a result, these assembled nanorods are constructed into ordered nanorod-based 3D nano-flowers. As the photocatalyst, the activity of these rutile $TiO_2$ nano-flower samples utilized in photocatalytic oxidation from benzylamine to imine would be examined.

Imine derivatives are very important starting materials in chemical industry to produce various value-added fine chemicals.[24] The conventional route to synthesize imines is from the condensation of amines and carbonyl compounds. However, it is often suffered from the low efficiency due to the over oxidation problems. Recently, an alternative route of the direct oxidation of amines was developed which offers a new strategy to produce imines, that is the photocatlytic conversion route based on $TiO_2$ photocatlysts.[25, 26] In this new method, $O_2$ or $O_2$ in the air was used as the oxidant, which makes the reaction facile and green. Usually, the selective photooxidation by $TiO_2$ in $H_2O$ is very hard to control due to its strong oxidation capability under UV light illumination, the products often end up to $CO_2$ and $H_2O$ for many organic reactants. However, it is been demonstrated that the highly selective oxidation by $TiO_2$ in $H_2O$ could be achieved by avoiding the generation of OH· radicals and unselective autooxidation.[27-30] And in the conversion of amines to imines by $TiO_2$ photocatalysts under visible light, an oxygenation pathway was demonstrated to be the key steps for this selective oxidation reaction, rather than the generation of

**Table 1** Photocatalytic reactivity for the oxidation of benzylamine to imine under visible light by rutile $TiO_2$ nano-flower and P25.

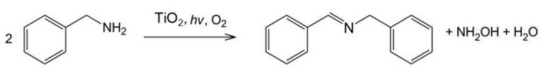


| | Conversion (%) | Selectivity (%) | Yield (%) |
|---|---|---|---|
| $TiO_2$ nano-flower-2h | 75.9 | 69.8 | 53.0 |
| $TiO_2$ nano-flower-4h | 99.9 | 73.3 | 73.2 |
| P25-2h | 33.0 | 68.1 | 22.5 |
| P25-4h | 78.1 | 73.0 | 57.0 |
| P25-6h | 98.7 | 73.6 | 72.6 |
| Blank | 0.78 | — | — |

OH· radical and autooxidation of amines in $H_2O$, thus high yield of imines could be achieved. Thus, the photo-reactivity of the rutile $TiO_2$ nano-flower catalysts was evaluated by photocatalytic oxidation of amines to imines. And in the meantime, P25 was the control sample, by which the reactions were conducted under the identical conditions, and the results were shown in Table 1. Benzylamine was used as the model compound for the selective oxidation process. N-benzylidenebenzylamine (N-BIBL) was the target product after the selective oxidation. The reaction results indicate that the rutile $TiO_2$ nano-flower catalysts exhibited superior activity than that of commercial P25 nano-powders. After 4 h reaction, the conversion of benzylamine by nano-flower catalysts approached to 99.9% and the selectivity to N-BIBL was 73.3%, so the total yield of N-BIBL achieved 73.2%. For the identical reaction time, the conversion of benzylamine by P25 only reached 78.1% and the yield of N-BIBL was only 57.0 %, which is much lower than that by single-crystalline rutile nano-flower catalysts. The reaction time was prolonged to 6 h, and the conversion by P25 finally achieved 98.7%, and the yield of N-BIBL was 72.6%. Besides, the blank experiment was also conducted, in which the yield of N-BIBL was examined under the identical reaction conditions without adding any photocatalyst. The conversion of benzylamine is extremely low (0.78%) in this control experiment, which addressed the significance of rutile $TiO_2$ nano-flower photocatalyst for remarkably promoting such selective oxidation reaction. The proposed mechanism for this selective oxidation reaction from amine to imine under visible light is illustrated in Scheme 2. At first, benzylamine was adsorbed on the surface of $TiO_2$, forming a complex, as shown in Scheme 2; this complex could act as the visible light absorber. Upon the excitation of visible light, photo-electrons and holes were generated; photo-generated holes could transfer to the substrate for the oxidation process, produce a free radical (Scheme 2), and electrons are retained in the lattice of $TiO_2$, generate Ti (III) center, so the effective separation of photo-generated charges is achieved. The photogenerated free radicals shown in

Scheme 2 could be easily oxidized by dioxygen dissolved in acetonitrile to generate benzaldehyde. At meantime, the electron in conduction band of $TiO_2$ would also complete the transfer to O species for the recovery of Ti(IV) center. After

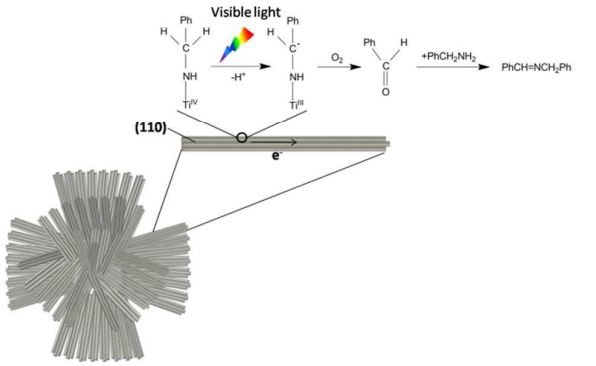


**Scheme 2**. Proposed mechanism for the generation of N-BIBL from benzylamine by rutile TiO2 nano-flower hierarchical structures under visible light irradiation.

this, the nucleophilic attack on benzaldehyde by the unreacted benzylamine would yield the corresponding N-BIBL. Thus the reaction occurred with high selectivity and high yield of target product. The enhanced photocatalytic activity of the rutile TiO2 nano-flower structure can be attributed to their three-dimensional (3D) hierarchical nanostructures and ordered single-crystalline rutile nanorods as the building blocks exposed (110) facets. 3D hierarchical nanostructures are usually considered to have advanced structures than 0D and 1D architectures because of the diffusion of active sites at different length scales on the surface of 3D nanostructures. And the single-crystalline rutile nanorods facilitate the vectorial transfer of the photo-generated electrons inside $TiO_2$ from conduction band to the surface active sites and shorten the mean diffusion length of the electrons (Scheme 2), this advanced nanostructure facilitate the charge separation and transfer, avoiding the excessive charge recombination which occurred in P25 due to randomness. So the rutile $TiO_2$ nanoflower exhibits superior activity in the oxidation process than P25. Furthermore, The complex of the 3D hierarchical nanostructures allow the multiple light reflections and scatterings, leading to improved light absorption by this nanostructure, all of these factors mentioned above resulted in the promotion of the reactivity by $TiO_2$ nano-flower structure in the selective photocatalytic oxidation from benzylamine to N-BIBL.

## Conclusions

To summarize, nano-flower like rutile $TiO_2$ hierarchical structures have been synthesized by a one-pot solvent-thermal method. And the building blocks of such nano-flower structures are single-crystalline rutile $TiO_2$ nanorods with their growth along [001] axis and exposed (110) facet on nanarods' side walls. Owing to this hierarchical nanostructure, this rutile $TiO_2$ displayed enhanced photocatalytic activity for the selective oxidation from benzylamine to N-BIBL. The results suggest the great potential of this 3D highly ordered hierarchical structure in photocatalytic fine chemical conversions. And this work offered the great opportunities to explore the promising prospect of the rational designed complex ordered nanostructures and their diverse applications in photocatalysis.

## Acknowledgements

This work was financially supported by the Singapore National Research Foundation (NRF-RF2009-04).

## Notes and references

1 B. O'Regan and M. Gratzel, *Nature*, 1991, **353**, 737.
2 A. Fujishima and K. Honda, *Nature*, 1972, **238**, 37.
3 (*a*) V. Subramanian, A. Karki, K. I. Gnanasekar, F. P. Eddy and B. Rambabu, *J. Power Sources*, 2006, **159**, 186. (*b*) Y. X. Tang, Y. Y. Zhang, J. Y. Deng, J. Q. Wei, H. L. Tam, B. K. Chandran, Z. L. Dong, Z. Chen and X. D. Chen, *Adv. Mater.*, 2014, **26**, 6111.
4 N. Wu, S. Wang and I. A. Rusakova, *Science*, 1999, **285**, 1375.
5 X. B. Chen and S. S. Mao, *Chem. Rev.*, 2007, **107**, 2891.
6 H. G. Yang, C. H. Sun, S. Z. Qiao, J. Zou, G. Liu, S. C. Smith, H. M. Cheng and G. Q. Lu, *Nature*, 2008, **453**, 638.
7 S.W. Liu, J. G. Yu andM. Jaroniec, *J. Am. Chem. Soc.*, 2010, **132**, 11914.
8 A. Selloni, *Nat. Mater.*, 2008, **7**, 613.
9 X. Y. Ma, Z. G. Chen, S. B. Hartono, H. B. Jiang, J. Zou, S. Z. Qiao and H. G. Yang, *Chem. Commun.*, 2010, **46**, 6608.
10 J. Fang, F. Wang, K. Qian, H. Z. Bao, Z. Q. Jiang and W. X. Huang, *J. Phys. Chem. C*, 2008, **112**, 18150.
11 B. Liu and E. S. Aydil, *J. Am. Chem. Soc.*, 2009, **131**, 3985.
12 X. J. Feng, K. Shankar, O. K. Varghese, M. Paulose, T. J. Latempa and C. A. Grimes, *Nano Lett.*, 2008, **8**, 3781.
13 E. Hosono, S. Fujihara and T. Kimura, *Electrochim. Acta*, 2004, **49**, 2287.
14 L. Xiao, Y. Yang, J. Yin, Q. Li and L. Zhang, *J. Power Sources*, 2009, **194**, 1089.
15 F. Lu, W. Cai and Y. Zhang, *Adv. Funct. Mater.*, 2008, **18**, 1047.
16 (*a*) X. F. Yang, J. L. Zhuang, X. Y. Li, D. H. Chen, G. F. Ouyang, Z. Q. Mao, Y. X. Han, Z. H. He, C. L. Liang, M. M. Wu and J. C. Yu, *ACS Nano*, 2009, **3**, 1212. (*b*) Y. Y. Zhang, Y. X. Tang, X. F. Liu, Z. L. Dong, H. H. Hng, Z. Chen, T. C. Sum, X. D. Chen, *Small*, 2013, **9**, 996.
17 X. F. Yang, J. Chen, L. Gong, M. M. Wu and J. C. Yu, *J. Am. Chem. Soc.*, 2009, 131, 12048.
18 X. F. Yang, C. J. Jin, C. L. Liang, D. H. Chen, M. M. Wu and J. C. Yu, *Chem. Commn.*, 2011, **47**, 1184.
19 W. G. Su, J. Zhang, Z. C. Feng, T. Chen, P. L. Ying and C. Li, *J. Phys. Chem. C*, 2008, **112**, 7710.
20 P. Chinnamuthu, A. Mondal, N. K. Singh, J. C. Dhar, K. K. Chattopadhyay and S. Bhattacharya, *J. Appl. Phys.*, 2012, **112**, 054315.
21 K. S. W. Sing, D. H. Everett, R. A. W. Haul, L. Moscou, R. A. Pierotti, J. Rouquerol and T. Siemieniewska, *Pure Appl. Chem.*, 1985, **57**, 603.
22 C. H. Wang, X. T. Zhang, C. L. Shao, Y. L. Zhang, J. K. Yang, P. P. Sun, X. P. Liu, H. Liu, Y. C. Liu, T. F. Xie and D. J. Wang, *J Colloid Interface Sci.*, 2011, **363**, 157.
23 P. M. Oliver, G. M. Watson, E. T. Kelsey and C. P. Stephen, *J. Mater. Chem.*, 1997, **7**, 563.
24 S. I. Murahashi, *Angew. Chem. Int. Ed. Engl.*, 1995, **34**, 2443.
25 X. J. Lang, H. W. Ji, C. C. Chen, W. H. Ma and J. C. Zhao, *Angew. Chem. Int. Ed.*, 2011, **50**, 3934.
26 X. J. Lang, W. R. Leow, J. C. Zhao and X. D. Chen, *Chem. Sci.*, 2015, **6**, 1075.
27 F. Parrino, A. Ramakrishnan and H. Kisch, *Angew. Chem. Int. Ed.*, 2008, **47**, 7107.
28 Y. Shiraishi, N. Saito and T. Hirai, *J. Am. Chem. Soc.*, 2005, **127**, 12820.
29 S. H. Zhan, D. R. Chen, X. L. Jiao and Y. Song, *Chem. Commn.*, 2007, 2043.
30 Q. J. Xiang, J. G. Yu and M. Jaroniec, *Chem. Commn.*, 2011, **47**, 4532.

Table of Contents

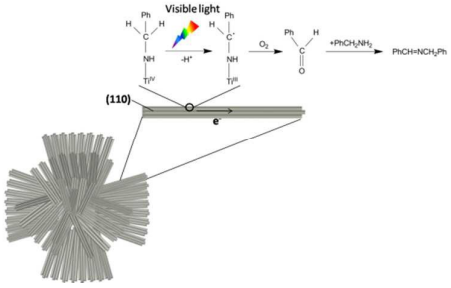


One-pot synthesized single-crystalline 3D rutile $TiO_2$ nano-flower hierarchical structures exhibited superior reactivity toward photocatalytic selective oxidation from amine to imine.